blood advances

American Society of Hematology
2021 L Street NW, Suite 900,
Washington, DC 20036
Phone: 202-776-0544 | Fax 202-776-0545
bloodadvances@hematology.org

Predicting inhibitor development using a random peptide phage-display library approach in the SIPPET Cohort

Tracking no: ADV-2023-011388R1

Shermarke Hassan (Leiden University Medical Center, Netherlands) Guido Baselli (Fondazione IRCCS Ca' Granda Ospedale Maggiore Policlinico, Italy) Luca Mollica (L.I.T.A/University of Milan, Italy) Riccardo Rossi (Bioinformatics, Istituto Nazionale Genetica Molecolare "Romeo ed Enrica Invernizzi", Italy) Himani Chand (University of Milan, Italy) Amal El-Beshlawy (Cairo University, Egypt) Mohsen Elalfy (Ain Shams University, Egypt) Vijay Ramanan (Jehangir Hospital Premises, Pune, India, India) Peyman Eshghi (Pediatric Congenital Hematologic Disorders Research Center, Research Institute for Childern's Health, Shahid Beheshti University of Medical Sciences, Tehran, Iran, Iran, Islamic Republic of) Mehran Karimi (American Hospital Dubai, United Arab Emirates) Roberta Palla (Università degli Studi di Milano, Italy) Frits Rosendaal (Leiden University Medical Center, Netherlands) Flora Peyvandi (Fondazione IRCCS Ca' Granda Ospedale Maggiore Policlinico,, Italy)

Abstract:
Inhibitor development is the most severe complication of hemophilia A care, and is associated with increased morbidity and mortality. The aim of this study was to use a novel IgG epitope mapping method to explore the factor VIII (FVIII)-specific epitope profile in the SIPPET cohort population and to develop an epitope-mapping based inhibitor prediction model. The population consisted of 122 previously untreated patients with severe hemophilia A that were followed-up for 50 days of exposure to FVIII or 3 years, whichever occurred first. Sampling was performed before FVIII treatment and at the end of the follow-up. The outcome was inhibitor development. The FVIII epitope repertoire was assessed by means of a novel random peptide phage-display assay. A LASSO regression model and a random forest model were fitted on post-treatment sample data and validated in pre-treatment sample data. The predictive performance of these models was assessed by the C-statistic and a calibration plot. We identified 27,775 peptides putatively directed against FVIII, which were used as input for the statistical models. The C-statistic of the LASSO and random forest models were good at 0.78 (95%CI: 0.69-0.86) and 0.80 (95%CI: 0.72-0.89). Model calibration of both models was moderately good. Two statistical models, developed on data from a novel random peptide phage display assay, were used to predict inhibitor development before exposure to exogenous FVIII. These models can be used to set up diagnostic tests that predict the risk of inhibitor development before starting treatment with FVIII.

Conflict of interest: COI declared - see note

COI notes: RP has received speaker fees from Novonordisk for an educational workshop. FP reports honoraria for speaking at educational meetings from Grifols and Roche and was a member of advisory boards for Sanofi, Sobi, Takeda, Roche, and Biomarin. SH, GB, LM, RLR, HC, AE-B, ME, VR, PE, MK, FRR declare no conflicts of interests.

Preprint server: No;

Author contributions and disclosures: SH, GB, LM, RLR and HC were involved in study design, manuscript development and analysis. RP, FP, and FR were involved in study design, data collection and manuscript development. AE, ME, VR, PE, MK, were involved in data collection and manuscript development.

Non-author contributions and disclosures: No;

Agreement to Share Publication-Related Data and Data Sharing Statement: Sequencing data generated and/or analyzed in this study are not publicly available due to containing sensitive clinical information but are available from the corresponding author upon reasonable request.

Clinical trial registration information (if any):

Predicting inhibitor development using a random peptide phage-display library approach in the SIPPET Cohort

Shermarke Hassan[1,2*], Guido Baselli[3*], Luca Mollica[4], Riccardo L. Rossi[5], Himani Chand[1], Amal El-Beshlawy[6], Mohsen Elalfy[7], Vijay Ramanan[8], Peyman Eshghi[9], Mehran Karimi[10], Roberta Palla[1], Frits R. Rosendaal[2], Flora Peyvandi[1,11]

[1]Università degli Studi di Milano, Department of Pathophysiology and Transplantation, Milan, Italy

[2]Department of Clinical Epidemiology, Leiden University Medical Center, Leiden, the Netherlands

[3]Fondazione IRCCS Ca' Granda Ospedale Maggiore Policlinico, Translational Medicine, Department of Transfusion Medicine and Hematology, Milan, Italy

[4]Department of Medical Biotechnologies and Translational Medicine, L.I.T.A/University of Milan, Milan, Italy.

[5]Bioinformatics, Istituto Nazionale Genetica Molecolare "Romeo ed Enrica Invernizzi", 20122, Milan, Italy

[6]Pediatric Hematology Department, Cairo University Pediatric Hospital, Cairo, Egypt

[7]Faculty of Medicine, Ain Shams University - Department Pediatrics, Cairo, Egypt

[8]Jehangir Clinical Development Centre, Department of Hematology, Jehangir Hospital Premises, Pune, India

[9]Congenital Pediatric Hematologic Disorders Research Center, Shahid Beheshti University of Medical Sciences, Tehran, Iran

[10]Pediatric Hematology-Oncology Department, American Hospital Dubai, Dubai, United Arab Emirates

[11]Fondazione IRCCS Ca' Granda Ospedale Maggiore Policlinico, Angelo Bianchi Bonomi Hemophilia and Thrombosis Center, Milan, Italy

*contributed equally

Correspondence address

Dr. F. Peyvandi

Università degli Studi di Milano

Department of Pathophysiology and Transplantation

Via Francesco Sforza 35, 20122, Milan, Italy

Tel: +39 0250320288

E-mail: flora.peyvandi@unimi.it

Manuscript information

Word count text:	3749
Figure/table count:	5 tables, 2 figures
Word count abstract:	248
Reference count:	44

Data sharing statement

Sequencing data generated and/or analyzed in this study are not publicly available due to containing sensitive clinical information but are available from the corresponding author upon reasonable request.

Keywords: hemophilia, inhibitor development, factor VIII, prediction

Key point

A novel random peptide phage display assay can be used to predict future inhibitor development before exposure to exogenous FVIII.

Abstract

Inhibitor development is the most severe complication of hemophilia A care, and is associated with increased morbidity and mortality. The aim of this study was to use a novel IgG epitope mapping method to explore the factor VIII (FVIII)-specific epitope profile in the SIPPET cohort population and to develop an epitope-mapping based inhibitor prediction model. The population consisted of 122 previously untreated patients with severe hemophilia A that were followed-up for 50 days of exposure to FVIII or 3 years, whichever occurred first. Sampling was performed before FVIII treatment and at the end of the follow-up. The outcome was inhibitor development. The FVIII epitope repertoire was assessed by means of a novel random peptide phage-display assay. A LASSO regression model and a random forest model were fitted on post-treatment sample data and validated in pre-treatment sample data. The predictive performance of these models was assessed by the C-statistic and a calibration plot. We identified 27,775 peptides putatively directed against FVIII, which were used as input for the statistical models. The C-statistic of the LASSO and random forest models were good at 0.78 (95%CI: 0.69-0.86) and 0.80 (95%CI: 0.72-0.89). Model calibration of both models was moderately good. Two statistical models, developed on data from a novel random peptide phage display assay, were used to predict inhibitor development before exposure to exogenous FVIII. These models can be used to set up diagnostic tests that predict the risk of inhibitor development before starting treatment with FVIII.

Introduction

Recent advances in the treatment of patients with hemophilia A (HA) have greatly improved clinical outcomes and quality of life. Nevertheless, one of the greatest treatment complications in severe hemophilia A is still the development of anti-factor VIII (FVIII) alloantibodies that neutralize FVIII (also called inhibitors). At least one third of patients treated with FVIII replacement therapy develop an inhibitor during the first 20-30 days of exposure to FVIII (EDs)[1], making treatment with FVIII ineffective. This in turn leads to increased morbidity and mortality among these patients. [1]

This complication is the result of a multi-causal immune response involving both patient- and treatment-related factors. [1] The type of FVIII product is one of the most important risk factors for inhibitor development, with the SIPPET randomized clinical trial showing that patients treated with recombinant FVIII (rFVIII) have an almost twofold higher risk of developing an inhibitor than those treated with plasma-derived FVIII (pdFVIII) products. [2] The pathophysiological mechanisms behind this increased immunogenicity remains unknown. Some plausible biological explanations have been postulated, such as the different post-translational modifications caused by the use of different cell lines during the manufacturing process of rFVIII products and the protective role played by Von Willebrand factor (VWF) in pdFVIII products. [3]

Mature FVIII consists of six major domains (A1, A2, B, A3, C1 and C2) and three acidic linking regions (a1, a2, a3); A1-a1-A2-a2-B-a3-A3-C1-C2. The VWF-FVIII complex forms through a high-affinity interaction between the FVIII light chain and the VWF D'D3 domains. [4] FVIII is activated by limited proteolysis through thrombin cleavage of three peptide bonds at Arg391 (a1-A2 junction), Arg759 (a2-B junction) and Arg1708 (a3-A3 junction). [5] After thrombin cleavage, activated factor VIII (without the B-domain) is released from VWF and binds to phosphatidylserine PS on the extracellular surface of activated platelets. [6,7]

The anti-FVIII humoral immune response is highly polyclonal and consists primarily of IgG antibodies recognizing variable multiple epitopes among patients and even in the same patient over time. [8] Several studies have examined the immunogenicity of FVIII and the mechanisms underlying inhibitor development during treatment with FVIII. [3,9,10] The role of FVIII B-cell epitopes in inhibitor development has been previously investigated using different techniques. Specific regions in the A2 (region encompassing Arg484-Ile508[11]), A3 (Gln1778-Asp1840[12]), C1 (Lys2065-Trp2212[13] and residues 2063-2071[14]) and C2 (residues Glu2181-Val2243[15] as well as other residues[16–18]) FVIII domains were shown to be target domains for FVIII alloantibodies interaction using several methods including low resolution immunoprecipitation, western blotting and antibody neutralization assays [8,19], as well as high resolution methods such as hydrogen–deuterium exchange mass spectrometry[18], crystallographic studies[20], surface plasmon resonance-based methods[17] and phage display [21–24].

In recent years, quantitative immunoproteomics has developed rapidly, offering high throughput analyses at relatively low cost. The aim of this study was to use a novel high-throughput epitope mapping technique based on a random peptide phage-display method in order to explore the overall FVIII epitope profile and to develop an epitope-mapping based inhibitor prediction model.

Methods

Patient population

Study samples were obtained from patients enrolled in the SIPPET trial, which was designed to investigate the immunogenicity of different FVIII products in patients with severe hemophilia A who were previously untreated with any FVIII concentrates (PUPs) or minimally treated with blood components. [2] Samples from 122 patients were used for this study. These patients were treated with 8 different FVIII products. (4 pdFVIII products and 4 rFVIII products) Inhibitor development was measured using the Bethesda assay with Nijmegen modification.[25] Thirty-nine out of 122 individuals developed an inhibitor.

One sample of citrated plasma was collected at baseline before exposure to FVIII (pre-treatment) and on sample at the end of the study (post-treatment). As previously described[2], in inhibitor-positive patients the end of the study was the time of inhibitor development. In inhibitor-negative patients the study ended when the patient reached 50 EDs or after three years of follow-up, whichever occurred first.

Approval for this study was obtained from the medical ethics committee at each study center and informed consent was obtained from all parents/guardians of patients.

Mimotope-variation analysis

Assay set-up

The total IgG epitope repertoire was assessed using mimotope-variation analysis (MVA), a phage display based method. (Protobios, Tallinn) as described previously. [26] A combinatorial library of randomized linear 12-mer peptides fused to the pIII minor coat protein of M13 phages (Ph.D.-12, New England Biolabs, UK) was used according to the manufacturer's protocol. Two µl of plasma was incubated with 5 µl of phage library (~5×10^{10} phage particles, overnight at +4 °C. The human immunoglobulin G (IgG)-captured phages were pulled down by protein G-coated magnetic beads (NEB, S1506S). Phage DNA was extracted, enriched and samples were barcoded by PCR amplification. Pooled samples were analyzed by Illumina sequencing (50-bp single end read, Genohub, USA). The resulting DNA sequences were *in silico* translated to 12 amino acid (aa) long peptide sequences. To correct for differences in sequencing depth among the samples, the total count of each unique peptide per sample was normalized in its counts per three million. The resulting output consisted of a database of 12-mer peptides with varying degrees of apparent affinity for IgG antibodies. In the context of the assay, apparent affinity was defined as the

frequency with which a 12-mer peptide was detected (i.e. the peptide count). These peptides are often referred to in the literature as “mimotopes”, due to the fact that they may mimic the structure of an epitope.

Two versions of the assay were performed, the standard MVA assay (described above) and a competition assay. In the MVA competition assay, the same factor VIII products that were used to treat the patient (Alphanate (Grifols), Fanhdi (Grifols), Emoclot (Kedrion Biopharma), Factane (LFB), Advate (Baxalta), Kogenate FS (Bayer AG), ReFacto AF (Pfizer) or Recombinate (Baxalta)) were also used to precondition study samples before competition analyses. In detail, respective FVIII products (final concentration: 3 uM) were incubated with 2 µl of plasma for 2 hours at room temperature before proceeding with the MVA assay as described above.

Removal of target unrelated peptides (TUPs)

One issue in conducting phage display experiments is the presence of so-called target-unrelated peptides (TUPs). These are false-positive results caused by selection-related TUPs which are peptides binding to materials and reagents used in the assay (for example, plastic surfaces, albumin), or propagation-related TUPs caused by faster propagation of some phage clones, resulting in a higher peptide count for some peptides. To minimize the effect of these TUPs, we removed all peptides that were predicted to be TUPs using the SAROTUP software tool. [27] Using this tool, known TUPs were filtered out exploiting the TUPscan and the mimosearch algorithms. Peptides with a high likelihood (P>0.8) to bind to polystyrene, as assessed by the PSBinder algorithm, were also filtered out.

Quality control using intra- and inter-assay replicates

To improve the assay signal to noise ratio, we focused on the most abundant peptides in the dataset. To establish an optimal abundance threshold, we relied on technical replicates of a control sample within the same MVA plate (intra assay) and across the different assay plates (inter assay). Each technical replicate was compared with its intra and inter assay littermates using each possible filtering threshold. As similarity metric, we accounted for the proportion of peptides in the dataset found in only one replicate at each possible threshold.

Identification of FVIII mimotopes

In order to find peptides identified using the MVA competition assay that bind selectively to FVIII-specific antibodies (FVIII mimotopes) the post-treatment sample was analyzed twice, once using the standard MVA assay and once using the MVA competition assay. FVIII mimotopes were defined as peptides that were present in the post-treatment sample in which the standard MVA assay was performed but not in the post-treatment sample in which the MVA competition assay was performed. Consequently, the abundance of each peptide in the standard MVA assay vs. the MVA competition assay was compared using the Fisher’s

exact test. Adjustment for multiple testing was done using the Bonferroni method. An adjusted p-value <0.05 was considered statistically significant. Only peptides significantly underrepresented in the MVA competition assay samples when compared to the standard MVA assay samples were considered to be FVIII mimotopes and used for further analyses.

Clustering workflow

Each FVIII epitope can be conceptualized as being represented by multiple peptide sequences, each containing the antibody-binding motif. Therefore, the Hammock algorithm, was used to cluster peptides based on sequence similarity before further analyses. [28] A complete linkage clustering algorithm was used for the initial clustering step. Cluster iterative merging was based on three iterations, maximum alignment length was set at 150% of that of the input peptide, 5% of the initial clusters were used as seeds for cluster merging. Applying the algorithm resulted in clusters of highly similar peptides. For each cluster, a consensus motif was generated based on the multiple sequence alignment of the sequences. Each consensus motif can be interpreted as representing an epitope motif. Highly conserved residues (>60%) were denoted with an uppercase symbol while moderately conserved residues (30%-60%) were denoted with a lower case symbol. Columns in the multiple sequence alignment where no single residue had a prevalence of >30% were denoted with "x". The total peptide count of each cluster was calculated as the sum of the count of each peptide included in a cluster. Clusters with an epitope motif that contained <4 conserved residues were filtered out from the dataset.

Alignment of epitope motifs to FVIII

Epitope motifs from the remaining clusters were then aligned to the linear amino acid sequence of FVIII (UniProt database ID: P00451). Local pairwise alignment using the Smith-Waterman algorithm was used. (R package: 'Biostrings' version 2.40.2) The degree to which a given residue on FVIII was surface accessible was calculated using the GETAREA algorithm[29] using as input the crystal structure of a B-domain deleted FVIII molecule[30] (PDB ID: 3CDZ). Based on the literature[31], a relative solvent accessibility of ≥ 20% was used a cut-off for defining whether a residue was buried or not.

Statistical analyses

Descriptive statistics

For the descriptive analyses, data was summarized using the mean and standard deviation (SD) or median and interquartile range (IQR), or as proportions.

Prediction modelling

To find biomarkers that were able to predict inhibitor development before the start of FVIII therapy, two statistical prediction models were fitted to the data. Both models were trained on data generated from the post-treatment samples, and were validated on data generated from the pre-treatment samples.

Firstly, a logistic regression model using L1 regularization (R package: 'glmnet' version 4.1.7), also called LASSO logistic regression, was evaluated using all clusters as the input. Leave-one-out cross-validation was used to select the optimal value for the regularization parameter. All clusters were used as the input for the model, the variables were centered and scaled before model fitting. Secondly. A random forest model (R package: 'randomForest' version 4.7-1.1) was evaluated using all clusters as the input. Values for the number of trees in the model and the number of variables at each split were selected by fitting models with different values of these parameters and then selecting the parameter value that minimized the out-of-bag error rate.

Evaluation of predictive performance

Predictive performance of these models was evaluated in two ways. Firstly, we assessed the degree to which a model could discriminate between patients with and without inhibitors, using an ROC curve. Secondly, we evaluated the degree to which the predicted cumulative incidence of inhibitor development matched the observed cumulative incidence using a calibration plot.

Selection of important clusters

To identify the clusters that were most important for inhibitor development, we first ranked the importance of each variable in the random forest model for model prediction by permutation feature importance. We then selected all the clusters with a feature importance score in the 90^{th} percentile. From this set, we then selected all the clusters that were also present (i.e. with a non-zero model coefficient) in the final LASSO regression model. We then generated descriptive statistics for this final set of clusters.

Approval for this study was obtained from the medical ethics committee at each study center and informed consent was obtained from all parents/guardians of patients.

Results

Mimotope Variation Analysis

Of the 122 previously untreated patients with hemophilia selected from the SIPPET study cohort for this analysis, 39 patients developed an inhibitor during follow-up (*Table 1*). Compared to inhibitor-negative patients, inhibitor-positive patients were slightly more likely to have a null mutation in the *F8* gene, and

slightly more likely to use a recombinant FVIII product, although these changes were not significant (*Table 1*).

The mean number of unique peptides generated from each patients' posttreatment samples was 356,365. After removing potential target-unrelated peptides, the mean number of unique peptides generated for each patient decreased to 313,340. As shown in Figure S1, both intra- and inter- assay- reproducibility started dropping when considering peptides with abundance < 250 reads. Therefore, only peptides found with abundance > 250 in at least one sample were considered for further analyses. This yielded 27,775 unique peptides that were identified as being FVIII mimotopes, with a median number of 266 (range: 4-1101) peptides per patient. These 27,775 peptides were then clustered (as described in the Methods section) which resulted in 223 clusters.

Location of clusters on FVIII

Using pairwise local alignment, 18 out of 223 clusters were mapped with acceptable alignment to the linear sequence of factor VIII. Most of these clusters were mapped against the B-domain (39%) (*Figure 1*). Of the 10 clusters that were mapped to parts of the linear sequence for which information on surface-accessibility was available, 9 were aligned to positions on FVIII that were partially surface-accessible (*Table 2*). All B-domain aligned peptide clusters had non-zero mean peptide counts in patients using a B-domain deleted product. Furthermore, Of the seven peptide clusters that were aligned to the B-domain, four peptide clusters had a higher mean peptide count among patients receiving treatment with full-length FVIIII compared to patients receiving B-domain deleted FVIII. (*Table 3*).

Predictive value of clusters

Next, we constructed two statistical prediction models to assess the degree to which the presence of these clusters in patients' samples were able to predict inhibitor development. First, a LASSO logistic regression model was fitted to all 223 clusters in the post-treatment patient samples. The fitted model was then used to predict inhibitor development using the pre-treatment patient samples. The C-statistic was 0.78 (0.69-0.86) (*Figure 2A*). Model calibration was good, as the cumulative incidence of inhibitor development predicted by the model was roughly in line with the observed incidence across the entire risk range (*Figure 2C*). Next, a random forest model was fitted to all 223 clusters in the post-treatment patient samples. The fitted model was then used to predict inhibitor development using the pre-treatment patient samples. The C-statistic was 0.80 (0.72-0.89) (*Figure 2B*). Model calibration was moderate, due to the model somewhat overpredicting the observed cumulative incidence of inhibitor development in the lower risk range (*Figure 2D*).

There were 12 clusters that had a feature importance score in the 90th percentile in the random forest model and were also part of the final LASSO logistic regression model (*Table 4*). Out of these 12 clusters,

only two mapped with good alignment to the linear sequence of FVIII. These two clusters were mapped to the A2 and A3 domain (*Table 4*). Ten out of twelve clusters had a higher peptide count in inhibitor-positive patients, compared to inhibitor-negative patients (*Table 4*). No clear differences were seen in the mean peptide counts of the clusters when measured in patients treated with plasma-derived FVIII versus patients treated with recombinant FVIII. *(Table 5)*.

Discussion

We assessed the FVIII-specific epitope profile of 122 previously untreated patients with hemophilia A, using a novel random peptide phage-display assay. Our results show that the apparent FVIII-specific antibody response is highly polyclonal, with many different epitope motifs. Among the 18 epitope motifs that were mapped to the linear sequence of FVIII, most of the mimotopes aligned with A1, A3 and B domain sequences. Using information on the presence of these epitope motifs in patient samples, two statistical prediction models (developed on post-treatment samples and validated in pre-treatment samples) were found to be predictive for inhibitor development.

Seven of the 18 epitope motifs (39%) with good alignment to FVIII were mapped to the B-domain. It is important to note that the alignments were not confirmed in-vitro (e.g. by antibody-binding assays using FVIII proteins with mutations at the relevant residues). All B-domain aligned peptide clusters had non-zero mean peptide counts in patients using a B-domain deleted product. This provides evidence against the hypothesis that the motifs of these peptide clusters truly represent targets of antibodies that are highly specific to a linear epitope on the B-domain. That being said, these results are based on very small numbers as there were only 7 patients using a B-domain deleted FVIII product (all Refacto).

Previous studies have suggested that antibodies against the B-domain might be predominantly of the non-neutralizing type [32–34], as the B-domain is not essential for the role of FVIII in blood clotting and is cleaved off after FVIII is activated. We could not verify this in our dataset as almost all epitope motifs that were most important for inhibitor prediction (*Table 4*) did not map well to the linear sequence of FVIII.

In the past, several studies have tried to develop models to predict inhibitor development. Most of these models were based on either clinical parameters (e.g. the age of FVIII treatment initiation, the type of FVIII product used or the intensity of the first treatment moment with FVIII) or genetic parameters (e.g. family history of inhibitor development, the type of *F8* gene mutation, HLA type or gene polymorphisms in immunoregulatory genes such as *IL10* or *CTLA4*). [35] Previously, a study in the SIPPET cohort also assessed the predictive value of the presence of non-neutralizing antibodies detected before treatment as part of a larger clinical prediction model for inhibitor development. [36] None of the aforementioned prediction models were able to accurately predict inhibitor development. In addition, some prediction models were only implementable after starting treatment with FVIII, due to the inclusion of treatment-related predictors

(e.g. information on treatment intensity can only be obtained after a couple of days of exposure to FVIII). This limits the applicability of these models as one would ideally want to have an idea about the risk of inhibitor development before FVIII treatment is initiated so that certain types of treatment modalities (e.g. exposure to exogenous FVIII) can be avoided. The models in this publication only use information on the pre-treatment epitope repertoire of the patient, and can therefore be used before FVIII treatment initiation.

The presence of peptides that specifically bind to anti-FVIII antibodies in samples taken before treatment with FVIII might seem unexpected at first glance. However, several studies have reported the presence of non-neutralizing anti-FVIII antibodies in healthy controls.[37] In addition, a previous study using pre-treatment samples of the current cohort reported that roughly 10% of patients had measurable anti-FVIII antibodies.[38] This suggests that natural autoreactivity against endogenous FVIII is relatively common in patients as well as healthy controls. Another hypothesis could be that the detected antibodies were not initially directed against FVIII, but were the result of previous exposure to a pathogen (e.g. a bacteria or virus) that contained a similar epitope. This cross-reactivity of the antibody response has been previously reported in several auto-immune disorders.[39] Our results indicate that the presence of anti-FVIII antibodies before treatment with FVIII might be a risk factor for inhibitor development in a subset of patients.

This approach has some limitations. Firstly, it has been shown that only a handful of contact residues within an epitope make a significant contribution to antibody binding. [40] In this study, we tried to identify these residues by clustering highly similar FVIII mimotopes and generating a consensus motif. Using alanine walk mutational analysis, the study by Kahle et al. [24] showed that there was reasonable agreement between a given consensus motif and the crucial binding residues of an epitope. Therefore, the consensus motifs derived from the multiple sequence alignment of each cluster of peptide sequences can, in theory, be considered to be potential epitope motifs. However, the accuracy of this approach is unknown and further verification is needed to identify the exact residues involved in binding to an antibody.

Secondly, the final epitope motifs were mapped to FVIII by aligning the motifs to the linear sequence of FVIII. However, it has been reported that the majority of B-cell epitopes are conformational. [41,42] (although the exact proportion of B-cell epitopes purported to be conformational is unknown) In this case, clustering based on sequence similarity might yield the correct conformational epitope motif, but the linear alignment procedure will produce faulty alignment. An alternative approach would involve mapping the epitope motifs to the three-dimensional structure of FVIII, using an in-silico approach. However, a recent study that assessed a set of B-cell epitope prediction algorithms against a benchmark dataset reported that all algorithms performed relatively poorly at mapping a potential epitope to the right location on an antigen. [43] That being said, knowing the correct location of these putative B-cell epitopes is not needed if the goal is only to predict inhibitor development.

We removed all peptides that were predicted to be target-unrelated (based on software exploiting publicly available repositories [27]) from the final peptide database. However, the residual impact of target-unrelated peptides that were not removed from the database on the results is difficult to quantify. In addition, some peptides can bind to both elements of assay as well as an IgG antibody. (i.e. they can be classified as both target-unrelated and target-related peptides) By removing these peptides, we might have inadvertently also removed some important peptides from the initial database.

From the output of the assay, only peptides with a count higher than 250 were selected, this resulted in a much smaller dataset. The cut-off was based on the intra- and inter-assay replicability (Figure S1). It is possible that many peptides that were the target of a FVIII-specific antibody were removed in this step.

Lastly, our analysis of the immune response did not include non-peptidic epitopes (such as the glycans present on the surface of FVIII). One difference between rFVIII and pdFVIII is in their respective glycosylation patterns. [44] Unfortunately, our approach does not allow assessment of the impact of differing glycosylation patterns on immunogenicity.

Conclusion

Two statistical models, developed on data from a novel random peptide phage display assay, were used to predict inhibitor development before exposure to exogenous FVIII. These models can be used to set up diagnostic tests that predict the risk of inhibitor development before starting treatment with FVIII.

Acknowledgements

This study was partially supported by the 2017 EAHAD Grant (awarded to Roberta Palla), 2017 Grifols investigator-sponsored research grant (awarded to Flora Peyvandi), the Italian Ministry of Health – Bando Ricerca Corrente 2020 (awarded to Flora Peyvandi) and by a Horizon 2020 Program grant (grant agreement ID: 859974, project name: EDUC8) Mimotope-variation analysis was performed by Protobios LLC.

Author Contributions

SH, GB, LM, RLR and HC were involved in study design, manuscript development and analysis. RP, FP, and FR were involved in study design, data collection and manuscript development. AE, ME, VR, PE, MK, were involved in data collection and manuscript development.

Conflict of interest statement

RP has received speaker fees from Novonordisk for an educational workshop. FP reports honoraria for speaking at educational meetings from Grifols and Roche and was a member of advisory boards for Sanofi,

Sobi, Takeda, Roche, and Biomarin. SH, GB, LM, RLR, HC, AE-B, ME, VR, PE, MK, FRR declare no conflicts of interests.

References

1. Peyvandi F, Garagiola I, Young G. The past and future of haemophilia: diagnosis, treatments, and its complications. *Lancet*. 2016;388(10040):187–197.

2. Peyvandi F, Mannucci PM, Garagiola I, et al. A Randomized Trial of Factor VIII and Neutralizing Antibodies in Hemophilia A. *N. Engl. J. Med.* 2016;374(21):2054–2064.

3. Cormier M, Batty P, Tarrant J, Lillicrap D. Advances in knowledge of inhibitor formation in severe haemophilia A. *Br. J. Haematol.* 2020;189(1):39–53.

4. Yee A, Oleskie AN, Dosey AM, et al. Visualization of an N-terminal fragment of von Willebrand factor in complex with factor VIII. *Blood*. 2015;126(8):939–942.

5. Pezeshkpoor B, Schreck U, Biswas A, et al. An in silico and in vitro approach to elucidate the impact of residues flanking the cleavage scissile bonds of FVIII. *PLoS One*. 2017;12(7):.

6. Lollar P, Parker CG. Subunit Structure of Thrombin-Activated Porcine Factor VIII. *Biochemistry*. 1989;28(2):666–674.

7. Van Dieijen G, Tans G, Rosing J, Hemker HC. The role of phospholipid and factor VIII(a) in the activation of bovine factor X. *J. Biol. Chem.* 1981;256(7):3433–3442.

8. Lollar P. Pathogenic antibodies to coagulation factors. Part one: Factor VIII and Factor IX. *J. Thromb. Haemost.* 2004;2(7):1082–1095.

9. Lai J, Hough C, Tarrant J, Lillicrap D. Biological considerations of plasma-derived and recombinant factor VIII immunogenicity. *Blood*. 2017;129(24):3147–3154.

10. Lacroix-Desmazes S, Voorberg J, Lillicrap D, Scott DW, Pratt KP. Tolerating Factor VIII: Recent Progress. *Front. Immunol.* 2020;10:2991.

11. Healey JF, Lubin IM, Nakai H, et al. Residues 484-508 contain a major determinant of the inhibitory epitope in the A2 domain of human factor VIII. *J. Biol. Chem.* 1995;270(24):14505–14509.

12. Barrow RT, Healey JF, Gailani D, Scandella D, Lollar P. Reduction of the antigenicity of factor VIII toward complex inhibitory antibody plasmas using multiply-substituted hybrid human/porcine factor VIII molecules. *Blood*. 2000;95(2):564–568.

13. Gish JS, Jarvis L, Childers KC, et al. Structure of blood coagulation factor VIII in complex with an anti–C1 domain pathogenic antibody inhibitor. *Blood*. 2021;137(21):2981–2986.

14. Batsuli G, Deng W, Healey JF, et al. High-affinity, noninhibitory pathogenic C1 domain antibodies are present in patients with hemophilia A and inhibitors. *Blood*. 2016;128(16):2055–2067.

15. Healey JF, Barrow RT, Tamim HM, et al. Residues Glu2181-Val2243 Contain a Major Determinant of the Inhibitory Epitope in the C2 Domain of Human Factor VIII. *Blood*. 1998;92(10):3701–3709.

16. Nguyen P-CT, Lewis KB, Ettinger RA, et al. High-resolution mapping of epitopes on the C2 domain of factor VIII by analysis of point mutants using surface plasmon resonance. *Blood*. 2014;123(17):2732–2739.

17. Lin JC, Ettinger RA, Schuman JT, et al. Six Amino Acid Residues in a 1200 Å2 Interface Mediate Binding of Factor VIII to an IgG4κ Inhibitory Antibody. *PLoS One*. 2015;10(1):e0116577.

18. Sevy AM, Healey JF, Deng W, et al. Epitope mapping of inhibitory antibodies targeting the C2 domain of coagulation factor VIII by hydrogen–deuterium exchange mass spectrometry. *J. Thromb. Haemost.* 2013;11(12):2128–2136.

19. Lavigne-Lissalde G, Rothschild C, Pouplard C, et al. Characteristics, mechanisms of action, and

epitope mapping of anti-factor VIII antibodies. *Clin. Rev. Allergy Immunol.* 2009;37(2):67–79.

20. Walter JD, Werther RA, Brison CM, et al. Structure of the factor VIII C2 domain in a ternary complex with 2 inhibitor antibodies reveals classical and nonclassical epitopes. *Blood*. 2013;122(26):4270–4278.

21. Villard S, Lacroix-Desmazes S, Kieber-Emmons T, et al. Peptide decoys selected by phage display block in vitro and in vivo activity of a human anti-FVIII inhibitor. *Blood*. 2003;102(3):949–952.

22. Villard S, Piquer D, Raut S, et al. Low molecular weight peptides restore the procoagulant activity of factor VIII in the presence of the potent inhibitor antibody ESH8. *J. Biol. Chem.* 2002;277(30):27232–27239.

23. Mühle C, Schulz-Drost S, Khrenov A V., et al. Epitope mapping of polyclonal clotting factor VIII-inhibitory antibodies using phage display. *Thromb. Haemost.* 2004;91(3):619–625.

24. Kahle J, Orlowski A, Stichel D, et al. Epitope mapping via selection of anti-FVIII antibody-specific phagepresented peptide ligands that mimic the antibody binding sites. *Thromb. Haemost.* 2015;113(2):396–405.

25. Duncan E, Collecutt M, Street A. Nijmegen-Bethesda assay to measure factor VIII inhibitors. *Methods Mol. Biol.* 2013;992:321–333.

26. Sadam H, Pihlak A, Jaago M, et al. Identification of two highly antigenic epitope markers predicting multiple sclerosis in optic neuritis patients. *EBioMedicine*. 2021;64:.

27. He B, Chen H, Li N, Huang J. Sarotup: A suite of tools for finding potential target-unrelated peptides from phage display data. *Int. J. Biol. Sci.* 2019;15(7):1452–1459.

28. Krejci A, Hupp TR, Lexa M, Vojtesek B, Muller P. Hammock: A hidden Markov model-based peptide clustering algorithm to identify protein-interaction consensus motifs in large datasets. *Bioinformatics*. 2016;32(1):9–16.

29. Fraczkiewicz R, Braun W. Exact and efficient analytical calculation of the accessible surface areas and their gradients for macromolecules. *J. Comput. Chem.* 1998;19(3):319–333.

30. Ngo JCK, Huang M, Roth DA, Furie BC, Furie B. Crystal Structure of Human Factor VIII: Implications for the Formation of the Factor IXa-Factor VIIIa Complex. *Structure*. 2008;16(4):597–606.

31. Savojardo C, Manfredi M, Martelli PL, Casadio R. Solvent Accessibility of Residues Undergoing Pathogenic Variations in Humans: From Protein Structures to Protein Sequences. *Front. Mol. Biosci.* 2021;7:.

32. Whelan SFJ, Hofbauer CJ, Horling FM, et al. Distinct characteristics of antibody responses against factor VIII in healthy individuals and in different cohorts of hemophili A patients. *Blood*. 2013;121(6):1039–1048.

33. Lebreton A, Lapalud P, Chambost H, et al. Prevalence and epitope specificity of non-neutralising antibodies in a large cohort of haemophilia A patients without inhibitors. *Thromb. Haemost.* 2011;105(6):954–961.

34. Vincent AM, Lillicrap D, Boulanger A, et al. Non-neutralizing anti-FVIII antibodies: different binding specificity to different recombinant FVIII concentrates. *Haemophilia*. 2009;15(1):374–376.

35. Bachelet D, Albert T, Mbogning C, et al. Risk stratification integrating genetic data for factor VIII inhibitor development in patients with severe hemophilia A. *PLoS One*. 2019;14(6):.

36. Hassan S, Palla R, Valsecchi C, et al. Performance of a clinical risk prediction model for inhibitor formation in severe haemophilia A. *Haemophilia*. 2021;27(4):e441–e449.

37. Abdi A, Bordbar MR, Hassan S, et al. Prevalence and incidence of non-neutralizing antibodies in congenital hemophilia a—a systematic review and meta-analysis. *Front. Immunol.* 2020;11:.

38. Cannavò A, Valsecchi C, Garagiola I, et al. Nonneutralizing antibodies against factor VIII and risk of inhibitor development in severe hemophilia A. *Blood*. 2017;129(10):1245–1250.

39. Rojas M, Restrepo-Jiménez P, Monsalve DM, et al. Molecular mimicry and autoimmunity. *J. Autoimmun.* 2018;95:100–123.

40. Novotny J. Protein antigenicity: A thermodynamic approach. *Mol. Immunol.* 1991;28(3):201–207.

41. Barlow DJ, Edwards MS, Thornton JM. Continuous and discontinuous protein antigenic determinants. *Nature*. 1986;322(6081):747–748.

42. Haste Andersen P, Nielsen M, Lund O. Prediction of residues in discontinuous B-cell epitopes using protein 3D structures. *Protein Sci.* 2006;15(11):2558–2567.

43. Sun P, Chen W, Huang Y, et al. Epitope prediction based on random peptide library screening: Benchmark dataset and prediction tools evaluation. *Molecules*. 2011;16(6):4971–4993.

44. Peyvandi F, Miri S, Garagiola I. Immune Responses to Plasma-Derived Versus Recombinant FVIII Products. *Front. Immunol.* 2021;11:.

Tables

Table 1. Patient characteristics.

	Inhibitor-negative (N=83)	Inhibitor-positive (N=39)
Age at first treatment (months)		
Mean (SD)	20.7 (17.6)	17.6 (13.0)
Family history of inhibitor development		
No	67 (80.7%)	31 (79.5%)
Yes	12 (14.5%)	4 (10.3%)
Unknown	4 (4.8%)	4 (10.3%)
F8 gene mutation (null vs. non-null)		
Non-null mutation	15 (18.1%)	1 (2.6%)
Null mutation	67 (80.7%)	35 (89.7%)
Unknown	1 (1.2%)	3 (7.7%)
F8 gene mutation (detailed)		
Frameshift mutation	10 (12.0%)	7 (17.9%)
Intron 1 inversion	4 (4.8%)	0 (0%)
Intron 22 inversion	32 (38.6%)	20 (51.3%)
Large deletion	5 (6.0%)	2 (5.1%)
Nonsense mutation	16 (19.3%)	6 (15.4%)
Missense mutation	8 (9.6%)	0 (0%)
Splice site mutation	4 (4.8%)	1 (2.6%)
Non-null mutation, type unknown	3 (3.6%)	0 (0%)
Unknown	1 (1.2%)	3 (7.7%)
FVIII product (type)		
Recombinant FVIII product	39 (47.0%)	22 (56.4%)
Plasma-derived FVIII product	44 (53.0%)	17 (43.6%)

Table 2. Linear alignment of mimotope clusters on FVIII

Mimotope core motif sequence	FVII sequence	Alignment	Residue number, start	Residue number, end	Domain	Nr of surface-accessible residues**
nxRRPfflnsg	LNSG	LNSG	187	190	A1	0
glggLi	LPGLI	L?GLI	261	265	A1	3
dPxqtll	QTLL	QTLL	316	319	A1	2
GLGqLL	LGQFL	LGQ?L	322	326	A1	4
nqkms	NQIMS	NQ?MS	583	587	A2	5
pdtppSxp	PPSMP	PPS?P	925	929	B	NA*
txxKtxIxTxt	TNRKTHI	T??KT?I	1028	1034	B	NA*
Ppdixspp	PPDAQNP	PPD???P	1105	1111	B	NA*
KVFRxp	KQFRLP	K?FR?P	1335	1340	B	NA*
VFRlpxtxt	FRLP	FRLP	1337	1340	B	NA*
TxltRtls	LTRVL	LTR?L	1423	1427	B	NA*
qNLsl	NLSL	NLSL	1461	1464	B	NA*
ydkadnerarlg	YDEDENQSPR	YD???N???R	1699	1708	other	NA*
dRxeLNmxxxl	RGELN	R?ELN	1768	1772	A3	3
lNEvLv	LNEHL	LNE?L	1771	1775	A3	3
hTnln	HTNTLN	HTN-LN	1878	1883	A3	4
kxDiLaxl	KVDLLA	K?D?LA	2091	2096	C1	3
KxDssGP	DSSG	DSSG	2150	2153	C1	3

*No information on surface-accessibility of B-domain and some adjacent residues.** The number of surface-accessible residues for each alignment was calculated using the GETAREA algorithm, as described in the Methods section.

Table 3: Mean peptide count (SD) of peptide clusters that were aligned to the B-domain, stratified by use of B-domain deleted or full-length FVIII.

	B-domain deleted FVIII (N=7)	Full-length FVIII (N=115)
qNLsl	175 (56.0)	349 (543)
KVFRxp	405 (627)	383 (948)
Ppdixspp	63.6 (89.0)	59.2 (288)
TxltRtls	119 (248)	1160 (10800)
txxKtxIxTxt	51.1 (63.3)	304 (1790)
VFRlpxtxt	157 (391)	395 (1870)
pdtppSxp	27.7 (27.4)	291 (716)

Table 4. Peptide clusters that were used as predictors in both the logistic regression model and the random forest classifier model.

Core motif	Mean peptide count in INH- Group	Mean peptide count in INH+ Group	Fold change	FVIII Domain	Number of unique peptides in cluster (%)	Peptide count of cluster (%)
kxPxstw	133	1826	13.70	-	24 (0.09%)	55764 (0.16%)
hntMels	38	119	3.10	-	11 (0.04%)	20460 (0.06%)
hTnln	151	454	3.01	A3	48 (0.17%)	66660 (0.19%)
nqkms	140	365	2.60	A2	31 (0.11%)	66660 (0.19%)
dxxYxlxm	438	1114	2.54	-	34 (0.12%)	63368 (0.18%)
Yvntxxxt	193	475	2.46	-	11 (0.04%)	25499 (0.07%)
LtqM	159	302	1.90	-	31 (0.11%)	61253 (0.17%)
pQyxnxxk	454	738	1.63	-	51 (0.18%)	52743 (0.15%)
sxnKP	325	483	1.49	-	53 (0.19%)	52537 (0.15%)
WDVpPxxxxt	301	445	1.48	-	21 (0.08%)	33105 (0.09%)
KxxHyxk	459	459	1.00	-	15 (0.05%)	39173 (0.11%)
qTAkfh	41	40	0.96	-	41 (0.15%)	48928 (0.14%)

Total number of unique peptides: 27775. Total peptide count: 35452858. -: Lack of good alignment on linear sequence of FVIII.

Table 5: Mean count of peptide clusters, stratified by inhibitor status, *F8* gene mutation and FVIII product type

	Inhibitor status				*F8* Gene mutation*		FVIII product type	
	Inhibitor-negative (N=83)	**Inhibitor-positive, total (N=39)**	**Inhibitor-positive, low-titer (N=15)**	**Inhibitor-positive, high-titer (N=24)**	**Non-null mutation (N=16)**	**Null mutation (N=102)**	**Recombinant FVIII product (N=61)**	**Plasma-derived FVIII product (N=61)**
Mean peptide count (SD)								
kxPxstw	133 (119)	1830 (9810)	4360 (15800)	240 (337)	145 (119)	779 (6070)	1190 (7850)	164 (196)
hntMels	38.5 (44.8)	119 (266)	256 (398)	33.4 (28.7)	88.5 (264)	61.6 (139)	91.8 (212)	36.6 (61.5)
hTnln	151 (372)	454 (1540)	850 (2370)	206 (564)	295 (590)	247 (985)	350 (1260)	145 (345)
nqkms	140 (199)	365 (1240)	168 (139)	489 (1570)	159 (215)	223 (784)	267 (996)	157 (223)
dxxYxlxm	438 (1590)	1110 (3850)	451 (840)	1530 (4850)	332 (440)	717 (2770)	889 (3140)	420 (1750)
Yvntxxxt	193 (290)	475 (891)	448 (523)	492 (1070)	185 (167)	299 (615)	286 (532)	280 (608)
LtqM	159 (483)	302 (1000)	159 (316)	391 (1250)	61.3 (106)	234 (752)	187 (797)	222 (573)
pQyxnxxk	454 (1170)	738 (1890)	109 (157)	1130 (2340)	176 (189)	614 (1560)	683 (1540)	407 (1320)
sxnKP	325 (674)	483 (858)	717 (995)	337 (746)	208 (293)	413 (794)	459 (888)	293 (543)
WDVpPxxxxt	301 (464)	445 (1130)	277 (277)	549 (1430)	331 (468)	358 (791)	330 (520)	364 (917)
KxxHyxk	459 (3120)	459 (1880)	99.5 (155)	684 (2380)	65.6 (164)	532 (3030)	617 (3630)	301 (1510)
qTAkfh	41.5 (103)	39.7 (82.9)	39.3 (97.9)	40.0 (74.3)	88.9 (164)	34.3 (81.9)	44.8 (104)	37.0 (88.6)

*4 patients were excluded from this analysis as their *F8* gene mutation was unknown.

Figure titles & legends

Figure 1

Title: Alignment of epitope motifs on the linear sequence of FVIII.

Legend: The plot shows the alignment of 18 epitope motifs on the linear sequence of FVIII. The X-axis represents the linear sequence of FVIII, from position 20 to 2,351. The Y-axis show a count for each position of the FVIII sequence. The count for each position was defined as the weighted sum of each cluster whose epitope motif was mapped to that position, using the peptide count of each cluster as weights. For example, if two clusters with a peptide count of 20 and 10 respectively, were mapped to a given position, then the total score for that position would be cluster 1 * 20 + cluster 2 * 10 = 30. The number of epitope motifs mapped to each domain, as a proportion of all 18 aligned epitope motifs, is shown at the bottom of the figure.

Figure 2

Title: Evaluation of the degree to which the logistic regression model and random forest classifier model can predict inhibitor development

Legend: Model discrimination (i.e. the degree to which a model assigns a higher risk to an inhibitor-positive patient versus an inhibitor-negative patient) was assessed by plotting ROC curves and by calculating the area under the curve (AUC). The AUC varies between 0.5 (no discrimination) to 1 (perfect discrimination). Figure 2A and 2B show the ROC curves of the LASSO logistic regression model and the random forest model respectively. Model calibration (i.e. the degree to which the predicted cumulative incidence of inhibitor development matched the observed cumulative incidence) was assessed using a calibration plot. For each quintile of predicted cumulative incidence, we plotted the mean predicted cumulative incidence of inhibitor development in a group against the observed cumulative incidence of inhibitor development in that group. In addition, we plotted a LOESS (Locally Estimated Scatterplot Smoothing) line in the same figure to assess model calibration across the full risk range. Ideally, all points should lie exactly on the diagonal line (which represents perfect agreement between predicted and observed values). Figure 2C and 2D show the calibrations plots of the LASSO logistic regression model and the random forest model respectively.

Figure 1

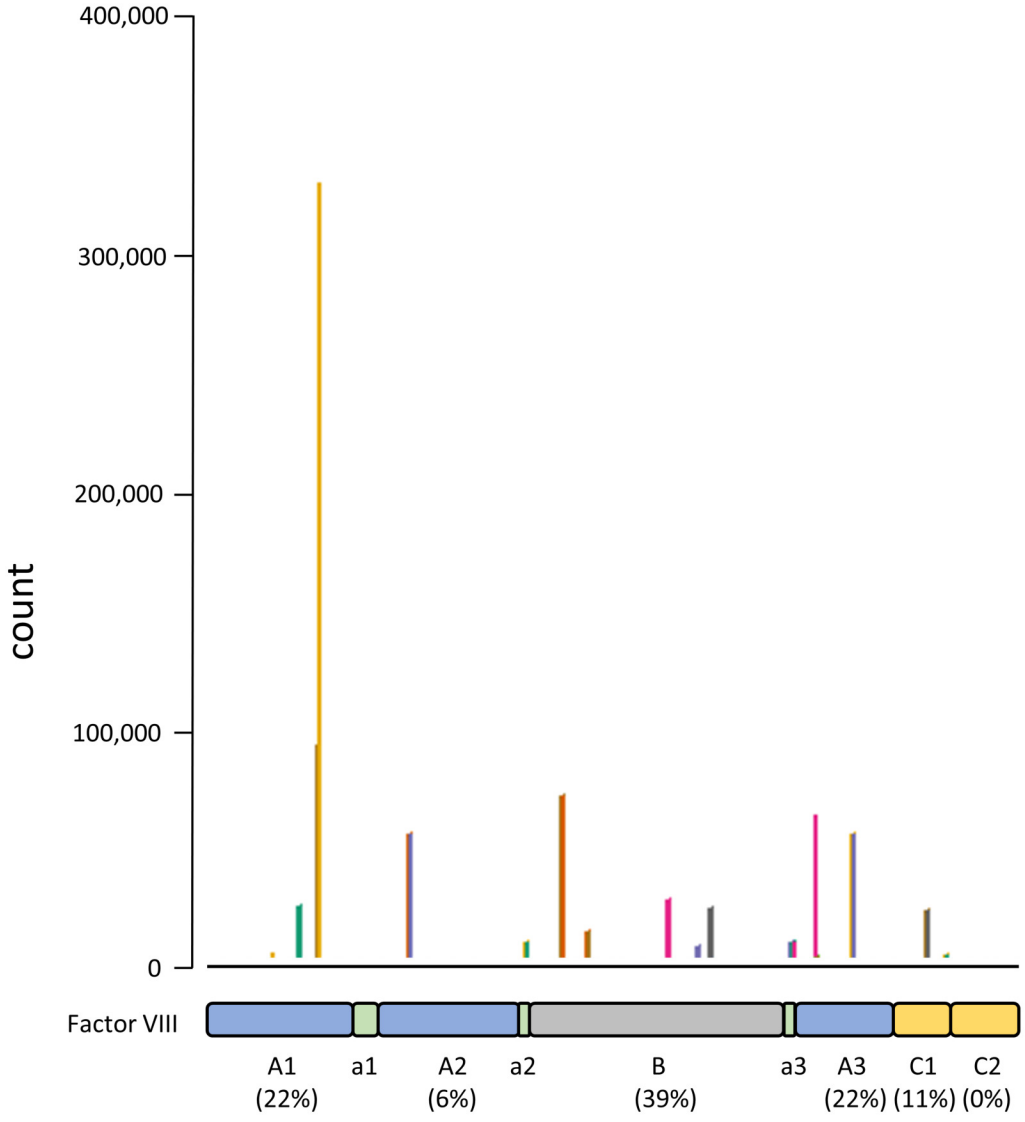

Figure 2